Fine Structure and Thermorheological Complexity of the Softening Dispersion in Styrene-Based Copolymers

Dino Ferri* and Leonardo Castellani

ENICHEM Research Center, Via Taliercio 14, 46100 Mantova, Italy

Received February 23, 2000

ABSTRACT: The segmental and terminal relaxation processes of polystyrene, styrene−acrylonitrile, and α-methylstyrene−acrylonitrile copolymers have been investigated by means of both dynamic-mechanical and dielectric spectroscopy in the linear response region. The temperature dependence of the average relaxation time τ of the two processes follows a Vogel−Tamman−Fulcher (VTF) equation: $\tau \propto \exp[B/(T - T_\infty)]$. Nevertheless, the segmental and terminal relaxations exhibit appreciably different VTF parameters. This vitiates time−temperature superpositioning in the segmental relaxation temperature region, giving rise to complex thermorheological behavior. As first shown by Plazek et al., this finding further confirms the Donth and Ngai models. Peculiar relationships between the VTF parameters of the segmental and terminal relaxation of the same polymer and of the same relaxation process of different polymers are pointed out. These relationships reveal general features of the VTF equation. A comparison between dynamic-mechanical and dielectric segmental relaxation times (τ_{mech} and τ_{diel}) highlights a profound difference in the time scales explored by the two techniques. More precisely, segmental motions contributing to the dielectric relaxation are faster than those observed mechanically. The relative magnitude of τ_{mech} and τ_{diel} was discussed using the DiMarzio−Bishop model. In addition, the ratio τ_{mech}/τ_{diel} is found to be temperature-independent. This suggests a scaling law for the decay function $\phi(t)$ of the segmental relaxation leading to the same temperature shift factors for different material properties.

Introduction

The study of the dynamics of polymer systems has made great strides in the past few years, and some features of their relaxation processes are now definitively recognized to be "universal".[1,2] When the molecular weight of a polymer exceeds a critical value M_c (which is often twice the entanglement molecular weight M_e), the softening dispersion exhibits two distinct dispersion zones which appear in different frequency ranges.[3] The high-frequency process, referred to as segmental relaxation (SR), involves only small chain segments, and its features are essentially molecular weight independent.[3] The low-frequency process, referred to as terminal dispersion or terminal relaxation (TR), involves diffusive motions of the whole chain along the tube of entanglement constraints determined by the neighboring chains. This process, usually described in terms of the reptation model,[4] is strongly molecular weight dependent and sensitive to molecular weight distribution and molecular topology. The temperature dependence of the mean relaxation time τ of both processes is generally described by the Vogel−Tamman−Fulcher (VTF) equation:[5−7]

$$\tau = \tau_0 \exp[B/(T - T_\infty)] \tag{1}$$

where B is a material parameter and T_∞ is called Vogel temperature. T_∞ can be considered as the temperature of a zero free volume state if the VTF equation is ideally extrapolated below T_g. This extrapolation can be physically meaningless, because evidences of a transition from VTF to Arrhenius behavior below the glass transition temperature of some polymers are reported in the literature.[36] The preexponent τ_0, corresponding to the relaxation time at infinite temperature, represents a microscopic dynamical quantity which can be interpreted as the inverse of an attempt frequency ω_0 for barrier crossing.[8] Usually eq 1 is used in the form

$$\omega = \omega_0 \exp[-B/(T - T_\infty)] \tag{2}$$

to fit the inverse relaxation time ω in a relaxation map, i.e., a plot of $\log(\omega)$ vs T^{-1}.

There is growing evidence in the literature that the VTF parameters of SR and TR differ for the same polymer,[9−12] and the first experimental evidence of such a phenomenology was reported in 1965.[30] The study of the segmental relaxation is often complicated by the presence of different molecular modes with different time scale, length scale, and temperature sensitivity determining its "fine structure".[9,13−15] A consequence of the fine structure is the breakdown of the time−temperature superposition principle (TTS) in the temperature region of the SR.[9,13−15] Several theoretical approaches to this phenomenology have been reported. Ngai et al. discuss the thermorheological complexity in terms of a coupling model,[11,16−18] while Donth et al. consider TTS breakdown as a necessary consequence of the preaveraging of the energy landscape of the longer modes due to the short modes.[9,13] Notwithstanding, some relationships between the VTF parameters of SR and TR seem to be of general validity. For instance, the Vogel temperature of the SR is always found higher than the TR one:

$$T_{\infty,SR} > T_{\infty,TR} \tag{3}$$

In view of these subtle "anomalies", careful and reliable measurements of the temperature dependence of the segmental and terminal relaxation times of different polymer systems are highly desirable to integrate the body of data already present in the literature. These measurements can further validate the predictions of these theoretical models contributing to give a consistent picture of polymer dynamics.

10.1021/ma000328c CCC: $20.00
Published on Web 05/05/2001

Table 1. M_w and M_w/M_n by GPC and T_g by DSC (Scanning Rate = 20 K/min) of the Samples Investigated

sample	$M_w \times 10^{-3}$	M_w/M_n	T_g (K)
PS	180	1.73	375.2
SAN	79	1.69	380.2
α-SAN	71.8	1.57	394.6

The aim of this paper is to carefully analyze the breakdown of TTS for polystyrene (PS), a styrene−acrylonitrile random copolymer (SAN), and an α-methylstryrene−acrylonitrile random copolymer (α-SAN). In particular, eq 3 will be verified, and the different mode sensitivity of two different activities, dynamic-mechanical analysis and dielectric spectroscopy, will be taken into account to enlarge the evidence of a fine structure of the softening dispersion of amorphous polymers.

Experimental Section

Three amorphous polymers were investigated: a polystyrene (commercial grade produced by EniChem), a styrene−acrylonitrile random copolymer (commercial grade produced by EniChem), and an α-methylstyrene−acrylonitrile random copolymer (produced by EniChem). These samples are characterized in Table 1. The glass transition temperatures were determined with a Perkin-Elmer DSC7 using thermograms on heating at 20 K/min, and the average molecular weight M_w and first polydispersity index M_w/M_n were determined by GPC calibrated with polystyrene standards.

Rubbery plateau modulus measurements were used to calculate M_e, and it was found that $M_w > 8M_e$ for the three samples. This value of M_w is high enough to establish a fully entangled network. This was verified comparing the T_g values of the samples investigated with those of higher M_w samples. No decrease of T_g was found due to the low molecular weight part of the MWD curve. This ensures that SR and TR are well separated.

Dynamic-mechanical analysis (DMA) was performed in shear with a Rheometrics mechanical spectrometer (RMS) model 800. The samples were compression-molded at about 470 K and recovered as rectangular 55 × 2 × 12 mm stripes or 25 mm diameter disks to fit the RMS tools. The linear viscoelastic functions have been measured using the rectangular torsion geometry in the SR temperature region and the parallel plate geometry (gaps ranging between 1 and 2 mm) in the TR temperature region. Isothermal frequency scans were performed in the range between 10^{-3} and 10^2 rad/s. The temperature was stable within 0.2 K over the range used in this study. Strain sweeps were previously performed to ensure that the viscoelastic response was linear, and time sweeps were also performed to test the thermal stability of all the samples in the TR temperature region. At the highest temperature investigated (533 K) no appreciable change of the viscoelastic functions was measured for times largely exceeding the time range necessary to perform the frequency sweeps. All tests were done under a N_2 atmosphere.

Frequency domain dielectric spectroscopy (DS) was performed by means of a spectrometer built by TNO (Netherlands Organisation for Applied Scientific Research) around a Schlumberger type 1250 frequency response analyzer. Specimens, in the form of compression-molded disks (thickness about 0.1 mm, diameter about 38 mm), were gold plated by vacuum sputtering.

Results and Discussion

A. Assessment of Segmental and Terminal Relaxation Times. In Figures 1, 2, and 3 the angular frequency dependence of the mechanical tan δ measured at several temperatures in the SR temperature region is shown for PS, SAN, and α-SAN. The tan δ peak

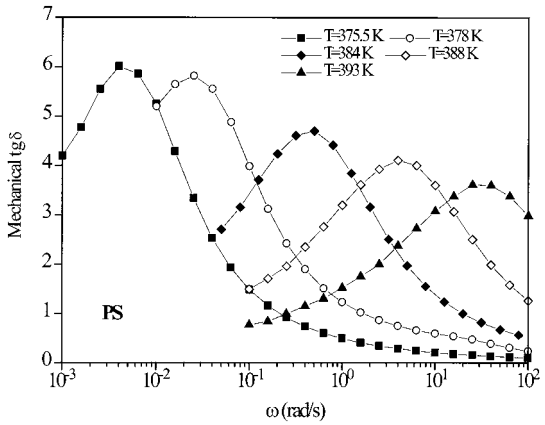

Figure 1. Angular frequency dependence of tan δ measured by DMA at several temperatures in the SR temperature region of PS.

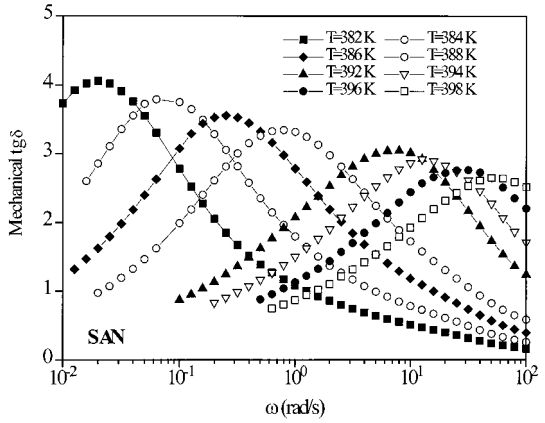

Figure 2. Angular frequency dependence of tan δ measured by DMA at several temperatures in the SR temperature region of SAN.

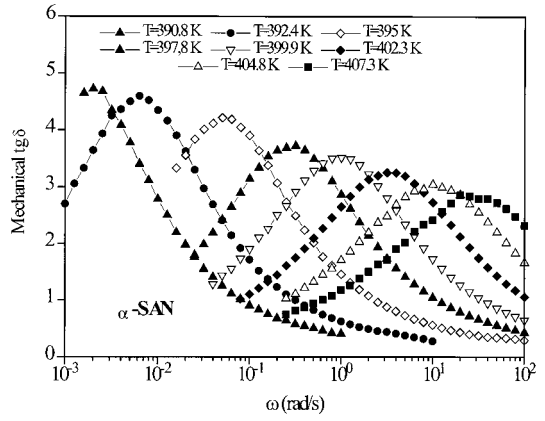

Figure 3. Angular frequency dependence of tan δ measured by DMA at several temperatures in the SR temperature region of α-SAN.

decreases and broadens with increasing temperature. As a consequence, the distribution of relaxation times is not simply shifted along the time axis when the temperature is changed, and TTS does not hold. This change in the viscoelastic behavior with temperature was first shown in 1968 by Plazek,[34] who observed a strong temperature dependence of the recovery curves of polystyrene. Thus, the idea to build a master curve in the SR temperature region cannot be taken into account. A possible criterion to calculate the segmental relaxation time is to consider the inverse of the angular

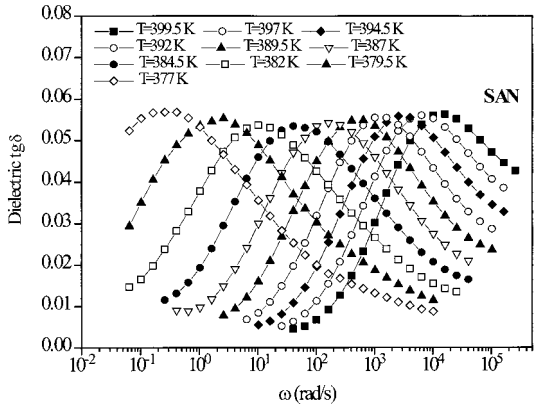

Figure 4. Angular frequency dependence of tan δ measured by DS at several temperatures in the SR temperature region of SAN.

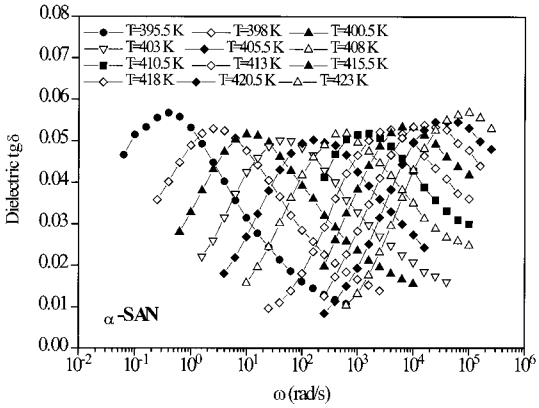

Figure 5. Angular frequency dependence of tan δ measured by DS at several temperatures in the SR temperature region of α-SAN.

frequency where the maxima of tan δ occur:

$$\tau = \frac{1}{\omega_{max}} \tag{4}$$

The relaxation times so calculated have the same temperature dependence as those estimated as the inverse of the angular frequency where the maxima of the loss shear modulus G'' occur. Equation 4 was also used to calculate the segmental relaxation times obtained by DS using the dielectric tan δ. The limited frequency range of the rheometers allows one to collect the τ values for a VTF fit only in a limited range of temperatures. Despite the efforts made to demonstrate the stability of the VTF parameters with respect to the experimental temperature range covered and/or the criteria adopted to calculate τ,[9] it is our opinion that reliable VTF parameters can be obtained only by enlarging, possibly with other experimental techniques, this temperature range. Because of the lack of dipole moments, both segmental and terminal modes of PS are nonactive dielectrically, and DS can be used in the SR region only for SAN and α-SAN. The presence of a dipole moment component perpendicular to the chain contour due to the CN− group makes the segmental relaxation dielectrically active in these two copolymers. In Figures 4 and 5 the angular frequency dependence of the dielectric tan δ measured at several temperatures in the SR temperature region is reported for SAN and α-SAN. The temperature range where the maxima can be seen with DS is clearly larger than that offered by DMA.

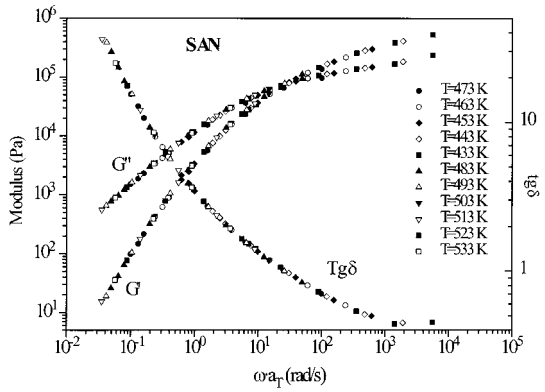

Figure 6. Master curve (referred at 473 K) of G', G'', and tan δ measured by DMA for SAN.

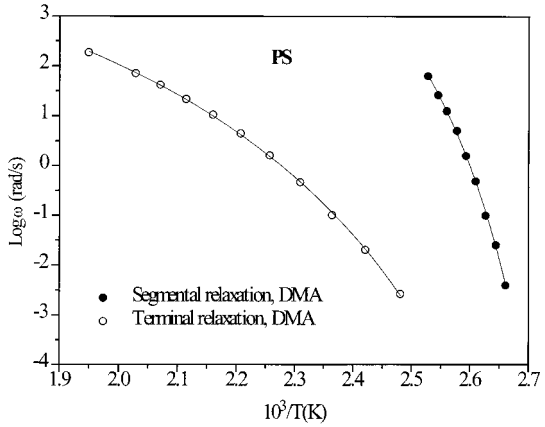

Figure 7. Arrhenius plot for the segmental and terminal relaxation of PS.

The situation for the TR is extremely more simplified because TTS was found to hold in the whole range of temperature investigated. As a typical example in Figure 6 a master curve for G', G'', and tan δ in the TR temperature region is reported for SAN (reference temperature 473 K). The reciprocal of the temperature-dependent crossover frequencies ω_c

$$\tau = \omega_c^{-1}|_{G'(\omega)=G''(\omega)} \tag{5}$$

between storage and loss shear moduli was used to calculate τ. In fact, the reciprocal of this angular frequency well agrees with the average relaxation time τ of the Fourier transformed slowed down exponential form of the stress relaxation modulus $G(t)$.[20]

B. VTF Coefficients for Segmental and Terminal Relaxation. Figures 7, 8, and 9 show the Arrhenius plot of the reciprocal relaxation time of PS, SAN, and α-SAN (determined with eqs 4 and 5) in the SR and TR temperature region. The VTF best fit curves (continuous lines) are reported and the best fit parameters are collected in Tables 2 and 3. In all the three cases the fit for the TR was done using a set of experimental points covering a temperature range of around 100 K. For the SR a temperature range of only 20 K is available for DMA results. Keeping the B parameter fixed at a value different from the best fit value in such a small temperature range, a difference of few degrees of T_∞ can easily compensate for a variation of a few hundred degrees for B in the best fit curve. Consequently, particular attention must be payed when considering

Table 2. Best Fit Parameters of the Mechanical VTF Eq 1 for the Segmental (SR) and Terminal (TR) Relaxation Processes Investigated by DMA

	SR				TR			
sample	log τ_0 (s)	B (K)	T_∞ (K)	$T_g - T_\infty$ (K)	log τ_0 (s)	B (K)	T_∞ (K)	$T_g - T_\infty$ (K)
PS	-8.4 ± 0.6	776 ± 100	344.7 ± 2	30.5 ± 2	-6.0 ± 0.1	1641 ± 80	320 ± 8	55.2 ± 3
SAN	-9 ± 1	937 ± 250	345.8 ± 5	34.4 ± 5	-6.5 ± 0.1	1750 ± 20	322.9 ± 1	57.3 ± 1
α-SAN	-9 ± 0.6	830 ± 90	360 ± 2	34.6 ± 2	-7 ± 0.1	2065 ± 70	316 ± 2	78.6 ± 2

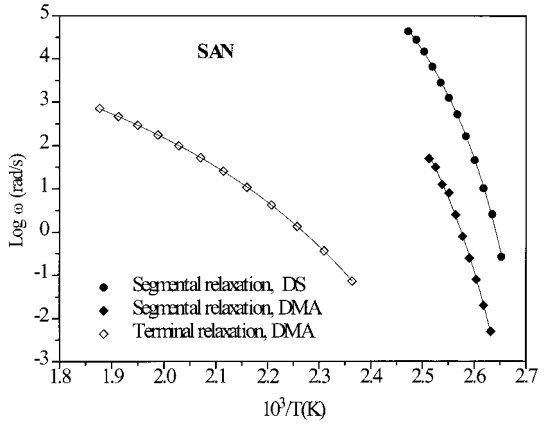

Figure 8. Arrhenius plot for the segmental and terminal relaxation of SAN.

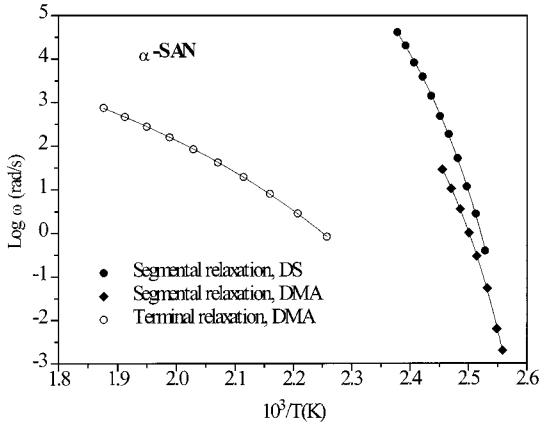

Figure 9. Arrhenius plot for the segmental and terminal relaxation of α-SAN.

Table 3. Best Fit Parameters of the Dielectric VTF Eq 1 for the Segmental (SR) Relaxation Process Investigated by DS

	SR			
sample	logτ_0 (s)	B (K)	T_∞ (K)	$T_g - T_\infty$ (K)
PS				
SAN	-10 ± 0.3	695 ± 50	348 ± 1	32.2 ± 1
α-SAN	-12 ± 0.4	950 ± 110	360 ± 2.5	34.6 ± 2

the reliability of the best fit VTF parameters calculated by DMA in the SR region. Nevertheless, our best fit VTF parameters for the SR of PS are in good agreement with those obtained by other authors over practically identical temperature ranges.[9,30] This is gratifying with regard to the reliability of the VTF parameters determined in the SR temperature region. In Figures 8 and 9 in the SR temperature region both the mechanical and the dielectric data are reported. It can be seen that DS enlarges the temperature range which can be used for the fit with the VTF equation.

Besides the reliability of the VTF parameters calculated for the SR, doubts could also arise concerning the validity of the VTF equation in the temperature region investigated. It is known in fact that an Arrhenius behavior can be encountered for some polymers in the vicinity of T_g and below it.[36] The lowest temperature T_L used to measure the tan δ peak (and to calculate τ) was in our case higher or slightly lower than the value of T_g reported in Table 1 ($T_L = T_g + 0.5$ K for PS, $T_L = T_g - 3$ K for SAN, and $T_L = T_g - 3.5$ K for α-SAN). The temperatures used to collect data for $T > T_L$ are in all cases above this T_g value. To investigate possible nonequilibrium effects (physical aging), the measurements at $T = T_L$ were repeated after keeping the sample at T_L for around 2 days, and no change in the viscoelastic curves was appreciated between annealed and nonannealed samples. The VTF curve was found to fit very well the whole body of data collected, included the low-temperature region points.

The data reported in Tables 2 and 3 show that the Vogel temperature values of the three polymers agree with eq 3. The same data also show that the value of B for the TR is more than doubled compared to that calculated for the SR. A comparison between B_{TR} and $T_g - T_{\infty,TR}$ and between B_{SR} and $T_g - T_{\infty,SR}$ (see Tables 2 and 3) suggests that the trend of B tracks that of the difference $T_g - T_\infty$. In other words, the TR exhibits both a greater B value and a greater $T_g - T_\infty$ value when compared to the SR.

C. Theoretical Approaches Explaining Different VTF Parameters for Segmental and Terminal Relaxation. In the literature the different activation parameters of the SR and TR have been explained in several theoretical frameworks.

Donth invokes a sort of preaveraging of the energy landscape of the slower (reptational) modes due to the faster (segmental) ones.[9,13] The two relaxation processes, both cooperative, possess different time and length scales. So the same monomeric units are involved in two distinct modes of relaxation. Each relaxation has its own energy landscape, and the long time scale process experiences a smoothed landscape, the smoothing being caused by a preaveraging due to the short time scale modes.[9,13] The VTF eq 1 states that only one temperature characterizes the relaxation: the Vogel temperature T_∞. Consequently, as a typical energy value defining the energy landscape roughness, it is reasonable to assume T_∞ multiplied by the Boltzmann constant: $E = kT_\infty$. The preaveraging of the energy landscape of the TR reduces E to a smaller value and necessarily leads to eq 3. A direct consequence of the preaveraging is a breakdown of TTS, because different modes with different temperature sensitivity, that is VTF parameters, contribute to the relaxation process in the SR temperature zone.

Ngai explains different temperature dependences of segmental and terminal relaxation and departure from TTS in the framework of the coupling model (CM).[1,21−23] In the CM the dynamics of a system is described by a coupling parameter n ($0 \leq n \leq 1$) correlated to the topological constraints experienced by a macromolecule due to the surrounding environment. The CM predicts for the temperature dependence of the observed friction

factor ζ the following equation:

$$\zeta(T) = [\zeta_0(T)]^{1/(1-n)} \tag{6}$$

where ζ_0 represents a primitive friction factor (of uncoupled relaxing units). Assuming the contribution of two different molecular processes to the SR and TR, their different nature leads to different coupling parameters, n_{TR} and n_{SR}. If the primitive friction factor for both process is the same, eq 6 states that TR and SR must exhibit different temperature dependencies. The assumption of a unique primitive friction factor for both processes is physically reasonable, because the definition of ζ_0 stems from a molecular basis in the CM. The CM states that in the SR temperature region the existence of different modes with different temperature sensitivity vitiates TTS and gives rise to thermorheological complexity.[16−18,22]

For the sake of completeness, we mention that evidence is also reported in the literature for a splitting of the viscoelastic relaxation spectrum of polymers into two components with different temperature dependences, named R and G.[26] The R component is well described in the frame of the Rouse theory, while the G component is responsible for relaxation from the high glassy modulus. The parallel contribution of the two components in the SR region leads, again, to thermorheologically complex behavior.

All these approaches present slightly different perspectives, but the concept of the different temperature sensitivity of different modes simultaneously contributing to the SR is the common argument used to explain TTS failure and different VTF parameters of the SR and the TR.

D. General Features of the VTF Parameters of SR and TR of a Polymer. A comparison between the VTF parameters of the SR and the TR *of the same polymer* points out some interesting features of the VTF behavior. As mentioned before, the values reported in Tables 2 and 3 are in agreement with eq 3. In addition, there is evidence that the VTF parameter B of the SR for each polymer is smaller than the corresponding value of the TR:

$$B_{SR} < B_{TR} \tag{7}$$

As previously mentioned and suggested by Donth, a preaveraging of the energy landscape of the TR can account for eq 3. The difference between the two Vogel temperatures stems in this framework from arguments relevant to the potential energy function of the system in its phase space. An interpretation of eq 3 in terms of free volume was first proposed by Plazek, who found puzzling results.[30] In the free volume theory one defines a fractional free volume f:

$$f = \frac{v - v_0}{v_0} \tag{8}$$

where v and v_0 are the total and occupied specific volumes. In addition, the fractional free volume f is assumed to have a linear temperature dependence:

$$f(T) = f_g + \alpha_f(T - T_g) \tag{9}$$

Table 4. Free Volume Parameters for PS

	SR	TR
v_0 (cm^3/g)	0.954	0.940
f_g (cm^3/g)	0.032	0.017
b	0.44	0.95

where $f_g = f(T_g) = (v_g - v_0)/v_0$ and

$$\alpha_f = \frac{1}{v_0}\frac{dv}{dT} \tag{10}$$

is the fractional free volume expansion coefficient. The Doolittle equation describes the free volume dependence of the relaxation time:

$$\tau = \tau_0 \exp(b/f) \tag{11}$$

Using eqs 9 and 11, it is possible to demonstrate that the VTF eq 1 holds and can be written in terms of free volume parameters as

$$\tau(T) = \tau_0 \exp\left[\frac{\frac{bv_0}{dv/dT}}{T - \left(T_g - \frac{f_g v_0}{dv/dT}\right)}\right] \tag{12}$$

Equation 12 states the relationships between the parameters B and T_∞ and the free volume ones:

$$v_0 = v_g - (T_g - T_\infty)\left(\frac{dv}{dT}\right) \tag{13}$$

$$b = \frac{B}{v_0}\left(\frac{dv}{dT}\right) \tag{14}$$

Following the idea of Plazek, one can set for PS v_g = 0.971 cm^3/g and $(dv/dT) = 5.5 \times 10^{-4}$ cm^3/(g K). These two quantities are a material property. Thus, they are unambiguously defined and the same for SR and TR. Under these reasonable assumptions, eq 13 states the intriguing result that different values of T_∞ for SR and TR of a polymer imply different occupied volumes for the two processes. This also leads to different fractional free volumes "seen" at T_g by the two processes. The values of v_0 and f_g obtained for the SR and TR of PS are reported in Table 4 and are in excellent agreement with those obtained by Plazek.[30] The necessity to invoke different occupied volumes *for the same polymer* compels one to reconsider the physical meaning of the free volume parameters. Plazek suggested that the smaller occupied volume of the TR is a time scale effect: the reptational modes are slow enough to have a greater probability (compared to the segmental ones) to experience density fluctuations. This leads to the equation

$$v_{0,SR} > v_{0,TR} \tag{15}$$

which expresses a similar concept as eq 3 in terms of free volume. Equation 15 also implies that the fractional free volume at T_g is smaller for the SR than for the TR:

$$f_{g,SR} < f_{g,TR} \tag{16}$$

Equation 14 allows one to interpret eq 7 in terms of free volume parameters. In fact, the increase of the B parameter for the TR implies that the product bv_0 is greater for the TR than for the SR. This, together with

eq 15, leads to the conclusion that not only

$$b_{SR} < b_{TR} \tag{17}$$

but also that the increase of the Doolittle exponent b for the SR must be stronger than the decrease of v_0. Both the b and B parameters determine the rate of decrease of the relaxation time with increasing fractional free volume or temperature. Starting from the experimental evidence that SR and TR have their own τ_0, B, and T_∞ it is possible to give a simple argument to understand why eqs 3 and 7 must be deeply correlated. Making the obvious physical requirement that $\tau_{TR}(T_g) > \tau_{SR}(T_g)$, one obtains the following relationship:

$$B_{TR} > (T_g - T_{\infty,TR})\left[\frac{B_{SR}}{T_g - T_{\infty,SR}} - \ln\left(\frac{\tau_{0,TR}}{\tau_{0,SR}}\right)\right] \tag{18}$$

Equation 18 imposes a limitation to the value which B can assume for the TR, and in the case of PS it leads to $B_{TR} > 1100$ K.

E. Comparison Between the VTF Parameters of SR and TR of Different Polymers. The values reported in Tables 2 and 3 reveal interesting features of the VTF parameters of the *same relaxation process* relevant to *different polymers*. One clear finding is that B tracks the trend of $T_g - T_\infty$ for both relaxation processes. In fact, focusing the attention on the SR, the relationships

$$B_{SR,PS} < B_{SR,SAN} < B_{SR,\alpha-SAN} \tag{19}$$

(found to hold within the experimental error) are coupled with the relationships

$$(T_g - T_{\infty,SR})_{PS} < (T_g - T_{\infty,SR})_{SAN} < (T_g - T_{\infty,SR})_{\alpha-SAN} \tag{20}$$

If we assume, following Donth's idea, that the VTF curve of the TR is modified by the preaveraging of the energy landscape, the relationships

$$B_{TR,PS} < B_{TR,SAN} < B_{TR,\alpha-SAN} \tag{21}$$

coupled with eq 19 suggest that the TR of the three polymers experience a similar preaveraging process.

The VTF behavior (and thus the VTF parameters) in the SR temperature region of a polymer is essentially dictated by the chemical structure, strength of coupling (value of the n parameter of Ngai), and magnitude of the glass temperature.[19] Alternatively, the "fragility" of a polymer chain (in the sense of Angell[8]) is the parameter determining the temperature dependence of the segmental relaxation time. The relationships in eq 21 highlight that the VTF parameter B of the TR also carries information concerning the polymer fragility. In fact, the difference between the B_{SR} values of different polymers is reflected in the VTF behavior of the viscosity and the terminal dispersion. The relationships

$$(T_g - T_{\infty,TR})_{PS} < (T_g - T_{\infty,TR})_{SAN} < (T_g - T_{\infty,TR})_{\alpha-SAN} \tag{22}$$

coupled with that given in eq 21 point out that B tracks the trend of $T_g - T_\infty$ also in the case of the TR.

The analysis of the ratio $B/(T_g - T_\infty)$ gives the cue to discuss another aspect of the VTF behavior which drew great attention in the past few years. Using eq 1, it is easy to demostrate that

$$\log\left(\frac{\tau_g}{\tau_0}\right) = \frac{B}{\ln 10(T_g - T_\infty)} \tag{23}$$

where τ_g is the relaxation time measured at $T = T_g$. Equation 23 states that the ratio $B/(T_g - T_\infty)$ is the number of orders of magnitude separating the relaxation time at infinite temperature and that at T_g divided by the factor ln 10. It has been proposed that this number of orders of magnitude is the same for the SR of all polymers.[8,35] This universality would explain all the relationships described by eqs 19 and 20. Data reported in Table 5 are consistent with this hypothesis which however cannot be validated here in view of the large uncertainties of the VTF parameters and the limited number of polymers investigated.

Table 5. Values of $B/(T_g - T_\infty)$ for the SR and TR Determined by DMA

	SR	TR
sample	$B/(T_g - T_\infty)$	$B/(T_g - T_\infty)$
PS	25 ± 3.5	30 ± 2.5
SAN	27 ± 7	30.5 ± 0.5
α-SAN	24 ± 2.5	26 ± 1

The data reported in Table 5 also show that the ratio $B/(T_g - T_\infty)$ is the same, within the experimental error, for SR and TR of each polymer. The constancy of τ_g/τ_0 (eq 23) could therefore be a general property of these relaxation processes, leading to the coupling between eqs 3 and 7.

F. Comparison Between Dynamic-Mechanical and Dielectric Responses. A direct and reliable comparison between mechanical and dielectric behavior of SAN and α-SAN can be done because the data reported were obtained for the same polymers in the same laboratory. In addition, the assessment of the dielectric and mechanical segmental relaxation time is done using the same criterion (eq 4) applied to directly comparable functions ($\tan\delta_{DMA}$ and $\tan\delta_{DS}$). The comparison gives the cue to discuss three subjects: TTS validity, magnitude and temperature dependence of DS, and DMA relaxation times.

We noticed previously that the curves of $\tan\delta$ measured by DMA do not follow TTS (see Figures 1−3). Figures 4 and 5 show that the body of data obtained by DS better follows TTS, even if subtle details imply a departure from TTS also for the DS data. Nevertheless, a higher quality master curve can be accomplished with the DS data rather than with the DMA ones as can be argued looking at Figures 10 and 11 where the two attempts at reduction for SAN have been reported to draw a comparison. For the reduction of the mechanical $\tan\delta$ the criterion used was to match the maxima.

Concerning the magnitude of the segmental relaxation times, one observes that, for a fixed temperature, the following relationship holds:

$$\tau_{mech} > \tau_{diel} \tag{24}$$

A behavior at odds with eq 24 was found by Pakula et al., by McKenna et al., and by Zorn et al. comparing the DS and DMA responses of polyisoprene[20] and polybutadiene,[24,37] respectively. However, in those cases the comparisons were drawn between the maxima of $\epsilon''(\omega)$ and $G''(\omega)$. We suggest that eq 24 is correlated with the fact that DS data better follow TTS than DMA ones.

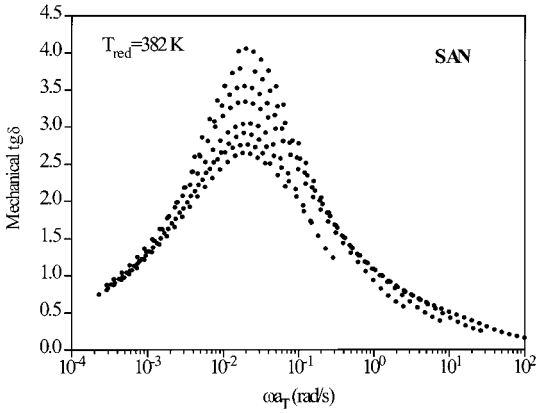

Figure 10. Master curve of tan δ (the criterion used was to match the maxima) measured by DMA for SAN.

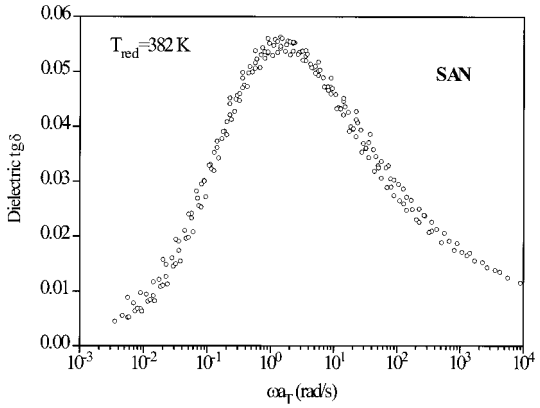

Figure 11. Master curve of tan δ measured by DS for SAN.

In fact, it suggests that dipoles relax on a length scale smaller than that of mechanically relaxing units, and thus the DS relaxation is not so strongly influenced by the entanglements. It cannot pass unnoticed that the gap betweeen τ_{mech} and τ_{diel} is very different for the two copolymers (around $2^1/_2$ decades for SAN and $1^1/_2$ decades for α-SAN). To qualitatively understand what this means and is due to, one needs a microscopic model relating DS and DMA measured quantities. A dielectric theory that explicitly includes viscoelastic parameters is that proposed by DiMarzio and Bishop (DB).[38] This is only one of the several proposed (for a comparison between the different models see ref 39). Obtained modifying the classical Debye theory of relaxation, the DB model predicts a relationship between the complex dielectric constant $\epsilon^*(\omega)$ and the complex modulus $G^*(\omega)$ of the form

$$\frac{\epsilon^*(\omega) - \epsilon_\infty}{\epsilon_0 - \epsilon_\infty} = \frac{1}{1 + KG^*(\omega)} \tag{25}$$

where K is a parameter given by

$$K = \frac{4\pi R^3}{kT}\left(\frac{\epsilon_0 + 2}{\epsilon_\infty + 2}\right) \tag{26}$$

In eq 26 R is the radius of a sphere containing the dipole moment, k is the Boltzmann constant, T is the absolute temperature, and ϵ_∞ and ϵ_0 are the instantaneous and equilibrium dielectric constant values, respectively. It has been shown that, given a particular complex modulus, increasing K, hence radius of the sphere, leads to an increase of the relaxation time of the dipoles.[39] It

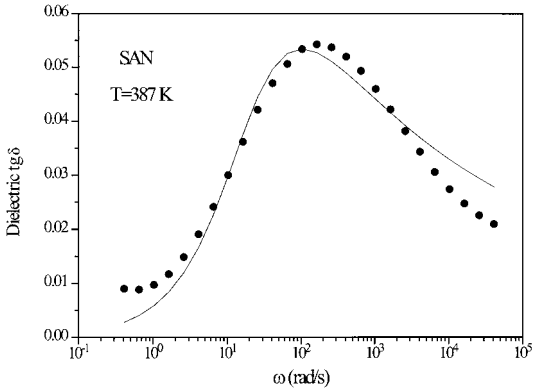

Figure 12. Test of the DB model for SAN. Points: dielectric loss tangent at 387 K. Line: best fit with the DB eq 27 from rheological dynamic moduli.

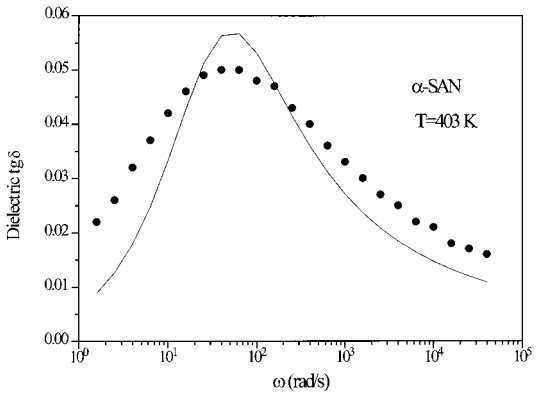

Figure 13. Test of the DB model for α-SAN. Points: dielectric loss tangent at 403 K. Line: best fit with the DB eq 27 from rheological dynamic moduli.

has also been shown that the DB model is oversimplified and does not accurately describe the relationship between viscoelastic and dielectric relaxation.[37] Despite this, Zorn et al. have shown that this model is able to qualitatively describe the physics underlying the relaxation processes. In fact, they were able to describe the measured increase of the ratio of dielectric and rheological relaxation times with increasing vinyl content of a series of polybutadiene samples in terms of different sphere radii of the dipoles.[37] To better understand the difference between τ_{mech}/τ_{diel} of SAN and α-SAN, we used the DB model to fit the dielectric relaxation at a fixed temperature with eq 25. To fit the dielectric tan δ, the real and imaginary parts of eq 25 must be calculated, and it is not difficult to demonstrate that the dielectric tan δ is given by

$$\tan\delta = \frac{KG''(\omega)}{\dfrac{A(\omega)}{(\epsilon_0/\epsilon_\infty) - 1} + [1 + KG'(\omega)]} \tag{27}$$

where

$$A(\omega) = [1 + KG'(\omega)]^2 + [KG''(\omega)]^2 \tag{28}$$

In eq 27 only K and $\epsilon_0/\epsilon_\infty$ were used as free parameters for the fit. Figures 12 and 13 report the best fit obtained for SAN at 387 K and for α-SAN at 403 K. It can be noticed that in both cases the DB model is not able to precisely infer the dielectric curve form the viscoelastic one. Nevetheless, the model is able to fairly well predict the position of the maximum of tan δ_{DS} on the angular

Table 6. Values of the Parameter *K* and of the Sphere Radius Containing the Dipole Moment Obtained for SAN and α-SAN from the DB Model

sample	K (GPa^{-1})	R (nm)
SAN	0.48	0.06
α-SAN	3.08	0.11

frequency axis. In Table 6 the best fit values of the parameter K are reported together with the sphere radii R calculated with eq 26 (the factor in parentheses was neglected because it was close to unity). The values of R are below the range expected for segmental relaxation and are consequently questionable. Even if the fit mismatch in Figures 12 and 13 calls for a refinement of the model, the results suggest that the dipole of SAN has a smaller effective sphere radius compared to that of α-SAN. In conclusion, the fact that the dipoles in α-SAN have to sweep a greater volume during relaxation can explain why the segmental DS relaxation times in α-SAN are more similar to the DMA ones. In other words, the length scales of DS and DMA relaxations are closer for α-SAN than for SAN. It should be also noticed that α-SAN has both a greater R and T_g value compared to those of SAN. This is what also Zorn et al. reported for polybutadiene.[37] It is maybe worth noting that this increase of R is associated not only with an increase of T_g but also with an increase of the B parameter of the VTF equation. This, according to the CM of Ngai, implies a greater coupling parameter for α-SAN with respect to SAN.

A third appealing feature emerges comparing the temperature dependence of τ_{mech} and τ_{diel} in an Arrhenius plot. Figures 8 and 9 highlight that the gap betweeen τ_{mech} and τ_{diel} is temperature-independent. This fact is proved also by the coincidence, within the experimental error, of the best fit values of both T_∞ and B obtained for the SR by DMA and DS (see Tables 2 and 3). This finding, reported also by Zorn et al. for polybutadiene,[37] suggests a scaling law for the correlation function $\phi(t)$ of the segmental relaxation of the form

$$\phi(t) = \chi\left[\frac{t}{\tau(T)}\right] \tag{29}$$

where χ is temperature-independent. Phenomenologies reminiscent of such a scaling law have been reported for the temperature dependence of the rotational correlation time of anisotropic organic molecules diluted in different polymers[25] used to test the dynamics of the polymer matrix on a well-defined length scale. The probe molecules exhibited a rotational correlation time whose temperature dependence was found to track that of the viscoelastic functions, which was much slower than the probes one. Recently, Faetti et al. studied the average rotational correlation time $\langle\tau\rangle$ of a paramagnetic tracer in PVAc.[29] They found a coupling between $\langle\tau\rangle$ and the segmental relaxation of the host matrix, revealed by the very good agreement between the values of B and T_∞ of the tracer and those obtained for PVAc by DS. Notwithstanding, they found that $\langle\tau\rangle$ is smaller than the segmental relaxation of the polymer matrix, the difference being more than 2 orders of magnitude. They interpret this as mainly due to the different length scales involved in the two processes.

Conclusions

The evidence of different activation parameters of segmental and terminal relaxation processes was enlarged to a new class of styrene-based random copolymers: styrene−acrylonitrile and α-methylstyrene−acrylonitrile. The investigation was performed using dynamic mechanical analysis and dielectric spectroscopy. A clear breakdown of time−temperature superpositioning was found in the segmental relaxation temperature region, and the theoretical frameworks accounting for this were reviewed. A comparison between the activation law parameters of the same relaxation process for different polymers was drawn, and a correlation between the VTF parameter B and the Vogel temperature T_∞ was pointed out.

The relationship ($B_{SR} < B_{TR}$) relating the VTF parameter B of the segmental and terminal relaxation processes of a polymer was highlighted, explained, and claimed to be of general validity.

A comparison between mechanical and dielectric response revealed that the two techniques are sensitive to different time and length scales. The values and temperature dependence of the dielectric and mechanical segmental relaxation times suggested a scaling property of the segmental relaxation process.

References and Notes

(1) Ngai, K. L. In *Disorder Effects on Relaxational Processes*; Richert, R., Blumen, A., Eds.; Springer: Berlin, 1994; p 89.
(2) Vilgis, T. A. In *Disorder Effects on Relaxational Processes*; Richert, R., Blumen, A., Eds.; Springer: Berlin, 1994; p 153.
(3) Ferry, J. D. *Viscoelastic Properties of Polymers*, 3rd ed.; Wiley: New York, 1980.
(4) Doi, M.; Edwards, S. F. *The Theory of Polymer Dynamics*; Clarendon Press: Oxford, 1986.
(5) Vogel, H. *J. Phisik Z.* **1921**, *22*, 645.
(6) Fulcher, G. S. *J. Am. Ceram. Soc.* **1925**, *8*, 339.
(7) Tammann, G.; Hesse, W. *Z. Anorg. Allg. Chem.* **1926**, *156*, 245.
(8) Angell, C. A. *Polymer* **1997**, *38*, 6261.
(9) Beiner, M.; Reissig, S.; Schröter, K.; Donth, E. J. *Rheol. Acta* **1997**, *36*, 187.
(10) Ngai, K. L.; Plazek, D. J. *J. Polym. Sci., Part B: Polym. Phys.* **1986**, *24*, 620.
(11) Alegria, A.; Macho, E.; Colmenero, J. *Macromolecules* **1991**, *24*, 5196.
(12) Plazek, D. J.; Zheng, X. D.; Ngai, K. L. *Macromolecules* **1992**, *25*, 4920.
(13) Donth, E. J. *Relaxation and Thermodynamics in Polymers. Glass Transition*; Akademie-Verlag: Berlin, 1992.
(14) Donth, E. J.; Beiner, M.; Reissig, S.; Koruss, J.; Garwe, F.; Vieweg, S.; Kahle, S.; Hempel, E.; Schröter, K. *Macromolecules* **1996**, *29*, 6589.
(15) Reissig, S.; Beiner, M.; Vieweg, S.; Schröter, K.; Donth, E. J. *Macromolecules* **1996**, *29*, 3996.
(16) Plazek, D. J.; Chay, I.-C.; Ngai, K. L.; Roland, C. M. *Macromolecules* **1995**, *28*, 6432.
(17) Ngai, K. L.; Plazek, D. J.; Rendell, R. W. *Rheol. Acta* **1997**, *36*, 307.
(18) Ngai, K. L.; Plazek, D. J.; Rizos, A. K. *J. Polym. Sci., Part B: Polym. Phys. Ed.* **1997**, *35*, 599.
(19) Plazek, D. J.; Ngai, K. L. *Macromolecules* **1991**, *24*, 1222.
(20) Pakula, T.; Geyler, S.; Edling, T.; Boese, D. *Rheol. Acta* **1996**, *35*, 631.
(21) Ngai, K. L.; Rendell, R. W.; Rajagopal, A. K.; Teitler, S. *Ann. N.Y. Acad. Sci.* **1986**, *484*, 150.
(22) Ngai, K. L.; Plazek, D. J. *J. Polym. Sci., Part B: Polym. Phys. Ed.* **1986**, *24*, 620.
(23) Roland, C. M. *Macromolecules* **1992**, *25*, 7031.
(24) McKenna, G.; Mopsik, F. I.; Zorn, R.; Richter, D. *Proc. ANTEC 97*.
(25) Inoue, T.; Cicerone, M. T.; Ediger, M. D. *Macromolecules* **1995**, *28*, 3425.
(26) Inoue, T.; Okamoto, H.; Osaki, K. *Macromolecules* **1991**, *24*, 5670.
(27) Cohen, M. H.; Turnbull, D. *J. Chem. Phys.* **1959**, *11*, 1164.
(28) Plazek, D. J. *J. Polym. Sci., Polym. Phys. Ed.* **1982**, *20*, 729.
(29) Faetti, M.; Giordano, M.; Leporini, D.; Pardi, L. *Macromolecules* **1999**, *32*, 1876.

(30) Plazek, D. J. *J. Phys. Chem.* **1965**, *69*, 3480.
(31) Plazek, D. J.; O'Rourke, V. M. *J. Polym. Sci., Part A-2* **1971**, *9*, 209.
(32) Plazek, D. J. *Polym. J.* **1980**, *12*, 43.
(33) Plazek, D. L.; Plazek, D. J. *Macromolecules* **1983**, *16*, 1469.
(34) Plazek, D. J. *J. Polym. Sci., Part A-2* **1968**, *6*, 621.
(35) Plazek, D. J.; Rosner, M. J.; Plazek, D. L. *J. Polym. Sci., Polym. Phys. Ed.* **1988**, *26*, 473.
(36) O'Connell, P. A.; McKenna, G. B. *J. Chem. Phys.* **1999**, *110*, 11054.
(37) Zorn, R.; Mopsik, F. I.; McKenna, G.; Richter, D. *J. Chem. Phys.* **1997**, *107*, 3645.
(38) DiMarzio, E. A.; Bishop, M. *J. Chem. Phys.* **1974**, *60*, 3802.
(39) Havriliak, S., Jr.; Havriliak, S. J. *J. Polym. Sci., Part B: Polym. Phys. Ed.* **1995**, *33*, 2245.

MA000328C